Cooperative Diversity in Wireless Networks: A Geometry-inclusive Analysis

Lalitha Sankaranarayanan
WINLAB, Dept. of ECE
Rutgers University
Piscataway, NJ 08854
lalitha@winlab.rutgers.edu

Gerhard Kramer
Bell Laboratories
Lucent Technologies
Murray Hill, NJ 07974
gkr@bell-labs.com

Narayan B. Mandayam
WINLAB, Dept. of ECE
Rutgers University
Piscataway, NJ 08854
narayan@winlab.rutgers.edu

Abstract

Cooperation between physically separated wireless nodes can achieve the high signal-to-noise ratio (SNR) diversity gains characteristic of multi-antenna arrays. Simulations indicate that such gains are still achieved for SNRs in the range of practical interest for several applications. Cooperation further yields *SNR gains* in addition to diversity gains. In contrast to diversity, the SNR gains are affected by the choice of inter-node distances. Such SNR gains are quantified in this paper via a geometry-inclusive error analysis. The notion of *geometry-inclusive SNR gains* is developed to facilitate geometry-based comparisons of cooperative strategies.

1 Introduction

In networks with nodes constrained in size and power, rate and diversity gains characteristic of multi-antenna arrays [1, 2] can be achieved via node *cooperation* [3–5]. Cooperation in communication networks results when terminals use their power, time, and bandwidth resources to mutually enhance their transmissions. The effect of cooperation is twofold: it achieves rate gains via shorter hops to cooperating neighbors or relays and it increases the spatial diversity available at the destination. Analogous to the analysis in [6] for multi-antenna networks, the benefits of cooperation can also be quantified via a diversity-multiplexing tradeoff analysis [4, 5]. In general, the tradeoff curve depends on both the number of cooperating nodes and the choice of cooperative strategy.

The diversity-multiplexing tradeoff analysis applies to quasi-static fading channels and gives a *limiting* relationship between error probability and achievable rate as a function of signal-to-noise ratio or SNR [6]. Numerical simulations further show that the predicted diversity gains can be achieved in the intermediate SNR ranges of practical interest for several applications [5, 7]. Cooperation also achieves *SNR gains* that are functions of the inter-node distances in this range. This means that certain sets of cooperating nodes can achieve the same diversity at a lower SNR than others. In contrast, the diversity-multiplexing tradeoff analysis ignores fixed quantities, such as path-gains, that do not scale with SNR. In order to quantify the distance-dependent SNR gains, we present a geometry-inclusive error analysis and define

This work is supported in part by the NSF under grants CCR-0429724, NeTS-0434854 and CCR-0325673.

a *geometry-inclusive SNR gain* to facilitate comparisons between cooperative strategies as a function of the network geometry. In [8], Laneman defines *coding gain* as the intercept of a log-outage vs. SNR in dB curve and evaluates it for specific cooperative diversity protocols at the maximum achievable diversity gain using a high SNR outage analysis. We here present a slightly more general geometry-inclusive approach that is valid for any diversity gain.

The paper is organized as follows. Section 2 presents a brief overview of the definitions and notations used. In Section 3, we define the geometry-inclusive SNR gain and illustrate the advantage of a geometry-inclusive error analysis for a fully cooperative m-source multi-access network. Such an analysis can be extended to networks employing cooperation. In Section 4, we present the coding gains for a cooperative network where the source nodes forward data for each other under the dynamic decode-and-forward (DDF) strategy [5]. Finally, in Section 5, we illustrate the SNR gains for a cooperative network via an example. The example motivates defining an *SNR threshold function* that characterizes the SNR range and corresponding inter-node distances over which the high SNR analysis is valid.

2 Preliminaries

The paper [6] presents a tradeoff between spectral efficiency and reliability as a function of the SNR ρ for a point-to-point wireless network with m transmit and n receive antennas. The network is modeled as having additive white Gaussian noise (AWGN) with block fading known only at the receiver (coherent model). The paper formalizes a relationship between the error probability and SNR via the notion of *exponential equality*. A function $f(\rho)$ is said to be exponentially equal to ρ^b, or $f \doteq \rho^b$, when

$$\lim_{\rho\to\infty} \frac{\log f(\rho)}{\log \rho} = b. \tag{1}$$

The value b is called the *exponential order* of $f(\rho)$.

Consider a family of codes $\{\mathcal{C}_\rho\}$, one for each ρ, such that $\mathcal{C}_\rho$ has a rate $R(\rho)$ bits/channel use and an average error probability $P_e(\rho)$. The family $\{\mathcal{C}_\rho\}$ is said to achieve a *spatial multiplexing gain* r and a *diversity gain* d if

$$r = \tfrac{R(\rho)}{\log \rho} \qquad \text{and} \qquad d(r) = \lim_{\rho\to\infty} \tfrac{-\log P_e(\rho)}{\log \rho} \tag{2}$$

i.e., we have $P_e(\rho) \doteq \rho^{-d(r)}$. The *diversity-multiplexing tradeoff* curve $d(r)$ thus quantifies an asymptotic dependence between P_e and SNR as the limiting slope of the $\log P_e$ vs. $\log \rho$ curve for the code family $\{\mathcal{C}_\rho\}$ [6].

3 Geometry-inclusive Error Analysis

Diversity analysis usually ignores the effect of geometry. However, the network geometry often plays a decisive role in the choice of cooperative strategy. In general, an analytic expression for the error probability is difficult to obtain for large multi-terminal networks. We can, however, sometimes obtain bounds on the error probability in the high SNR regime that preserve the limiting diversity-multiplexing tradeoff while allowing geometry-based comparisons.

Throughout this paper, we use the following standard notations [9]. Let f and g be functions of a continuous variable $\rho \in \mathcal{R}$. We write

$$\begin{array}{lll} f = O(g) & \text{if } |f(\rho)| \leq A\,|g(\rho)|\,, & |\rho| > \rho_o \\ f = o(g) & \text{if } |f(\rho)| \leq \varepsilon\,|g(\rho)|\,, & \forall \varepsilon > 0 \text{ and } |\rho| > \rho_1(\varepsilon) \\ f = \Theta(g) & \text{if } A_1\,|g(\rho)| \leq |f(\rho)| \leq A_2\,|g(\rho)|\,, & |\rho| > \rho_o \\ f \sim g & \text{if } \lim_{\rho\to\infty} \frac{f(\rho)}{g(\rho)} = 1 & \end{array} \tag{3}$$

where A, A_1, A_2, and ρ_o are positive constants and $\rho_1(\varepsilon)$ is a positive function of the positive valued ε.

Let $\mathcal{N}_j(\underline{d}^{(j)})$ represent a network of M_j nodes with internode distances $d_{mk}^{(j)}$, $m = 1, 2, \ldots,$ M_j, $k = 1, 2, \ldots, M_j$, $m \neq k$, collected in the vector $\underline{d}^{(j)}$. We assume that all nodes have the same transmit power and the same noise variance. For each $\underline{d}^{(j)}$, we define a vector of *exponential orders* $\underline{\Delta}^{(j)}(\rho) \triangleq -\alpha \log \underline{d}^{(j)} / \log \rho$, where $\alpha > 1$ is the path-loss exponent. Observe that for finite non-zero $d_{mk}^{(j)}$, we have, $\lim_{\rho\to\infty} \underline{\Delta}^{(j)}(\rho) = 0$. Each network chooses a communication strategy characterized by a family of codes $\{\mathcal{C}_\rho^{(j)}\}$ such that the j^{th} network achieves the diversity-multiplexing tradeoff $d_j(r)$. We denote the high SNR geometry-inclusive error probability for the j^{th} network by $P_e^{(j)}$.

For any communication strategy, we approximate the error probability as

$$P_e \sim (c(R, \underline{d}) \cdot \rho)^{-d(r)} \tag{4}$$

where $c(R, \underline{d})$ is a coding gain (see [8]). Let $P_e^{(j)}$ be the error probability of network $\mathcal{N}_j$ when using a predefined communication strategy. We define the *SNR gain* of network $\mathcal{N}_1$ over network $\mathcal{N}_2$ as follows.

Definition 1 *The SNR gain ρ_{gain} in dB of $\mathcal{N}_1(\underline{d}^{(1)})$ over $\mathcal{N}_2(\underline{d}^{(2)})$ that achieves the same diversity gain $d(r) > 0$ at a multiplexing gain r is*

$$\rho_{gain} = \frac{10}{d(r)} \lim_{\rho\to\infty} \log_{10} \frac{P_e^{(2)}(\rho, \underline{d}^{(1)})}{P_e^{(1)}(\rho, \underline{d}^{(2)})} \tag{5}$$

We motivate the need for a geometry based formulation by considering a cooperative network of m nodes that transmit to a destination (node $m+1$) where the transmitting nodes can fully cooperate. Since the m nodes are in general at different distances from the destination, we call this network an $m \times 1$ *distributed* MIMO (multi-input, multi-output) network. The received signal at the destination over l channel uses is

$$\underline{Y} = \begin{bmatrix} \frac{h_1}{\sqrt{d_1^\alpha}} & \frac{h_2}{\sqrt{d_2^\alpha}} & \cdots & \frac{h_m}{\sqrt{d_m^\alpha}} \end{bmatrix} X + \underline{Z} \tag{6}$$

where X is an $m \times l$ matrix with complex entries x_{kj}, $k = 1, 2, \ldots, m$, $j = 1, 2, \ldots, l$, transmitted in the j^{th} symbol by the k^{th} source over a channel with gains h_k. The h_k are assumed to be realizations of independent and identically distributed (i.i.d) proper, complex Gaussian random variables and we write the corresponding random variables as $H_k \sim \mathcal{CN}(0, 1)$. The distance vector $\underline{d}$ has as its k^{th} entry the distance $d_{k,m+1}$ between the k^{th} source and the destination. We write the corresponding vector of exponential orders as $\underline{\Delta}$ with entries Δ_k, for all

k. The additive noise vector $\underline{Z}$ has i.i.d proper complex Gaussian entries $Z_j \sim \mathcal{CN}(0,1)$ such that the SNR from each antenna at the destination is ρ. We use upper case letters to denote random variables (X) and the corresponding lower case letters (x) to denote a realization of the random variables.

The channel gains are assumed known at the receiver but not at the transmitter and the channel is assumed to be constant over a coherence time greater than the block length l, where $l >> 1$. We define

$$V_k = \frac{\log 1 \,/ |H_k|^2}{\log \rho} \tag{7}$$

that has the probability density function

$$p(v_k) = \ln(\rho)\, \rho^{-v_k} e^{-\rho^{-v_k}}. \tag{8}$$

We have

$$p(\cdot) = \begin{cases} o(\rho^{-v_k} \ln \rho) & v_k < 0 \\ \Theta\left(\rho^{-v_k} \ln \rho\right) & v_k \geq 0 \end{cases} \tag{9}$$

where A_1 and A_2 are e^{-1} and 1 respectively. The minimum outage probability P_{out} for a family of codes $\{\mathcal{C}(\rho)\}$ with rate R is thus

$$P_{out}(R) = \Pr(I(X;Y|\underline{h}) < R = r\log\rho) = \Pr\left\{\log\left(1 + \sum\nolimits_{k=1}^{m} \rho^{(1+\Delta_k - v_k)}\right) < R\right\} \tag{10}$$

where $I(X;Y|\underline{h})$ is the maximum rate achievable when $\underline{H} = \underline{h}$ is known only at the destination. $P_{out}(R)$ in (10) can be computed analytically. However, to compute the SNR gains it suffices to write (10) as

$$P_{out}(R) \sim \Pr(\rho^{\max_k (1+\Delta_k - v_k)^+} < \rho^r) \sim c' \left(\prod\nolimits_{k=1}^{m} d_{k,m+1}^{\alpha}\right) \rho^{-m(1-r)} = c' \rho^{-m(1-r) - \sum_{k=1}^{m} \Delta_k} \tag{11}$$

where $c' > 0$ is a positive constant independent of ρ and $\underline{d}$. The dominant SNR term, obtained using (9), is that with the smallest exponent in the outage region $O_{out}^{+} = \{\underline{v} \succeq 0 : \max_k (1+\Delta - v_k)^+ < r\}$ where $(x)^+ = \max(x,0)$ and $\succeq$ denotes that every entry of $\underline{v}$ is positive. For the case where the $d_{k,m+1}$ are distinct, P_{out} can be evaluated to show that $c' = 1/m!$.

The average error probability P_e is

$$P_e = P_{out}(R) P(\text{error}|\text{outage}) + P(\text{error, no outage}). \tag{12}$$

We assume that for large l, $P(\text{error, no outage})$ is negligible while $P(\text{error}|\text{outage})$ is almost one. We thus have $P_e \sim P_{out}$ with the coding gain $c(R,\underline{d})$ given as

$$c(R,\underline{d}) = \left(C \cdot \prod\nolimits_{k=1}^{m} d_{k,m+1}^{\alpha}\right)^{\frac{-1}{m(1-r)}} \tag{13}$$

where C is a positive constant independent of R and $\underline{d}$.

The following example demonstrates the effect of geometry on the SNR gains. Consider two $m \times 1$ distributed MIMO networks $\mathcal{N}_1(\underline{d}^{(1)})$ and $\mathcal{N}_2(\underline{d}^{(2)})$. From (5), we have

$$\rho_{gain} = \frac{10}{d(r)} \lim_{\rho\to\infty} \log_{10} \frac{\left(\prod_{k=1}^{m} d_{k,m+1}^{(2)}\right)^{\alpha} \rho^{-m(1-r)}}{\left(\prod_{k=1}^{m} d_{k,m+1}^{(1)}\right)^{\alpha} \rho^{-m(1-r)}} = \frac{10\alpha}{m(1-r)} \sum_{k=1}^{m} \log_{10} \frac{d_{k,m+1}^{(2)}}{d_{k,m+1}^{(1)}} \tag{14}$$

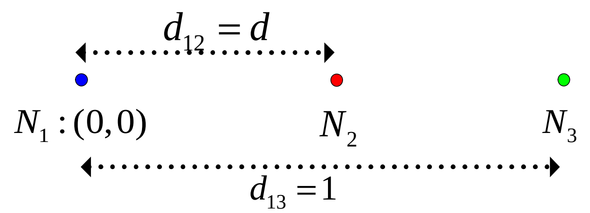

Figure 1: A 2×1 Distributed MIMO Network

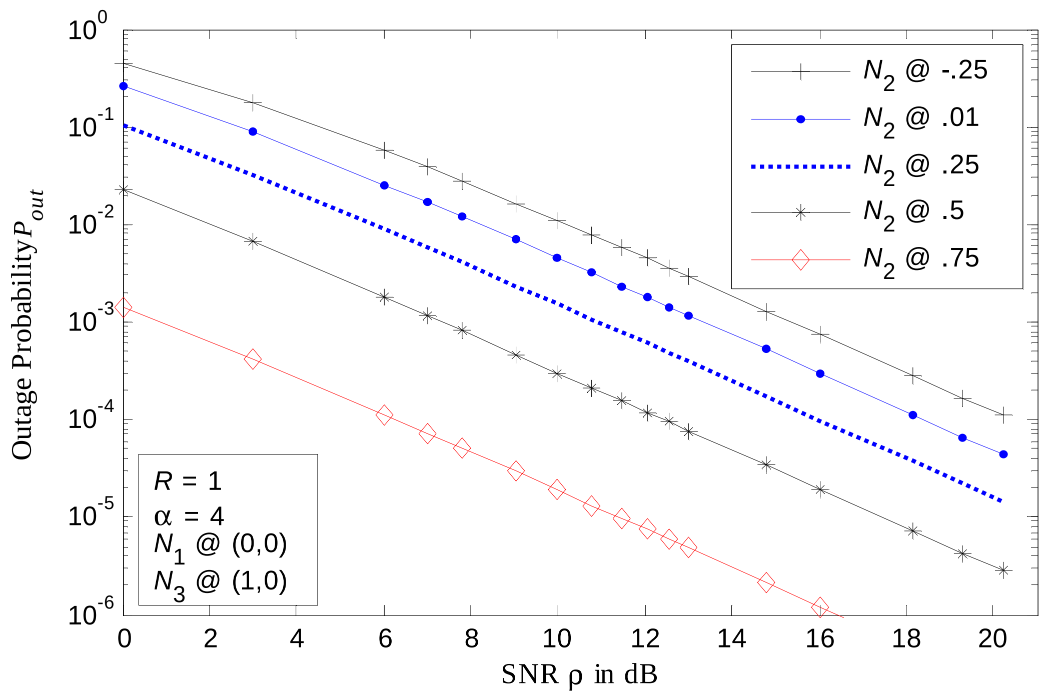

Figure 2: P_{out} for a 2×1 Distributed MIMO Network

For example, for an $m = 2$ fully cooperative network with $d_{1,3}^{(1)} = d_{1,3}^{(2)}$, $d_{2,3}^{(2)} = 2d_{2,3}^{(1)}$, and $\alpha = 4$, $\mathcal{N}_1$ enjoys an SNR gain of 6 dB relative to $\mathcal{N}_2$ at $r = 0$. We illustrate this further by considering a 2×1 MIMO network with a collinear geometry as shown in Fig. 1 where node N_1 is fixed at the origin a unit distance from the destination node N_3 while node N_2 is at a variable distance d from N_1. The nodes N_1 and N_2 transmit with the same average power such that their SNR at N_3 is ρ. In Fig. 2, for $R = 1$ and $\alpha = 4$, we plot the outage probability curves for the 2×1 distributed MIMO network as a function of ρ in dB, one for each choice of d. The curves are plotted using the closed form outage expression for the 2×1 distributed MIMO network. As expected, the SNR gains between any two choices of d, even over the relatively low SNR range chosen, match exactly those predicted in (14) with increasingly larger SNR gains achieved as N_2 moves closer to N_3. The above example, albeit simple, serves to demonstrate the technique used to evaluate the asymptotic geometry-inclusive error probability. One can similarly compare the error performance of any two networks that achieve the same $d(r)$. In the following section, we present $C(R, \underline{d})$ and ρ_{gain} for a cooperative network under the DF strategy.

4 Cooperative Networks

4.1 Network Model

We consider a cooperative network consisting of M source nodes numbered $1, 2, \ldots, M$ and a destination node $M + 1$. We write $\mathcal{S} = \{1, 2, \ldots, M\}$ and $\mathcal{S}_{\mathcal{C}} = \mathcal{S} \cup \{M + 1\}$ to denote, respectively, the set of source nodes and all nodes in the network. Associated with this network is a distance vector $\underline{d}$, with $\binom{n}{2}$, $n = |\mathcal{S}_{\mathcal{C}}|$, entries of inter-node distances where $|\mathcal{S}_{\mathcal{C}}|$ is the cardinality of the set $\mathcal{S}_{\mathcal{C}}$. The corresponding vector of exponential orders, $\underline{\Delta}$, has entries Δ_{km} for all $k, m \in \mathcal{S}_{\mathcal{C}}$, $k \neq m$. We write $\kappa_{km} \triangleq 1 + \Delta_{km}$. Unless otherwise stated, all nodes have the same power constraint, have a single antenna, and have a half-duplex (HD) transmit-receive constraint.

4.2 Cooperative Networks

Azarian et al in [5] obtained the tradeoff curve for an M-source cooperative network under a time-division multi-access (TDMA) constraint on the sources. They consider a dynamic DF (DDF) strategy where each time-duplexed source, during its transmission, is aided sequentially by the remaining $(M-1)$ sources acting as HD relays. Thus each source uses a total of M slots to complete its transmission. The DDF strategy, like the DF strategy for the HD relay channel, allows both non-orthogonal source transmissions and unequal transmit-receive channel use at the relay [10, 11]. However, as the name suggests, it allows each cooperating node or relay to dynamically adjust the duration of its receive state until sufficient energy is collected to successfully decode the transmitted message. Finally, this duration assumed known at the destination.

In [7], we present a partial decode-and-forward (PDF) strategy for the cooperative network where the sources transmit their messages using orthogonal subchannels (TDMA) but use the same subchannel (MAC) to cooperatively forward to the destination. We refer to this scheme as a TDMA-MAC scheme. The PDF strategy generalizes the DF strategy by considering an additional message stream at each source that is decoded only by the destination. For simplicity, we consider the DF strategy here where all source messages are decoded by the other sources. Since each transmitting source is aided by the remaining $(M - 1)$ sources simultaneously only in the MAC slot, the TDMA-MAC scheme is equivalent to a two-slot TDMA scheme where each transmitting source is aided by $(M - 1)$ sources simultaneously in the second slot. For the case where all source nodes transmit at the same rate $R = r \log \rho$, the symmetric $d(r)$ for this strategy is given by the following theorem.

Theorem 1 *The diversity-multiplexing tradeoff $d(r)$ for a cooperative network employing the DF strategy under the TDMA-MAC scheme is*

$$d(r) = \begin{cases} M(1-r) & r \in \left[0, \frac{1}{M}\right] \\ \frac{1}{r} - 1 & r \in \left[\frac{1}{M}, 1\right] \end{cases} \tag{15}$$

Sketch of Proof: The cooperative network under the TDMA-MAC scheme simplifies to one where each time-duplexed source is aided simultaneously by $(M - 1)$ relays. The $d(r)$ analysis is then similar to that in [5] for the DDF strategy.

We remark that the $d(r)$ above is *uniformly dominated* by the $d(r)$ for the TDMA scheme in [5]; i.e., $d_A(r) \leq d_B(r)$ where A and B are the TDMA-MAC and TDMA schemes respectively. The uniform dominance of the latter is a result of the temporal diversity available at the destination via the M source-destination paths versus only two in the former. The advantage of the TDMA-MAC over the TDMA scheme, however, is that it allows a simple and tractable geometry-inclusive error analysis. The corresponding $c(R,\underline{d})$ is then given by the following theorem. Define $\kappa_m^{(\mathcal{C})} \triangleq \min_{k\in\mathcal{S},m\neq k}\kappa_{mk}$ with equivalent distance $d_{m,(\mathcal{C})}$ and $d_{m,av} = \prod_{k\in\mathcal{S},m\neq k} d_{k,M+1}^{1/(M-1)}$.

Theorem 2 *The geometry-inclusive coding gain for the m^{th} source in the cooperative network employing the DF strategy under the TDMA-MAC transmission scheme is*

$$c_m(R,\underline{d}) = \begin{cases} \left(C\cdot\prod_{k=1}^{M} d_{k,M+1}^{\alpha}\right)^{\frac{-1}{M(1-r)}} & r\in\left[0,\frac{\kappa_m^{(\mathcal{C})}}{M}\right] \\ \left(C\cdot d_{m,M+1}^{\alpha}\right)^{\frac{-1}{M(1-r)}}\cdot\left(\frac{1}{d_{m,(\mathcal{C})}^{\alpha}\cdot d_{m,av}^{\alpha}}\right) & r\in\left[\frac{\kappa_m^{(\mathcal{C})}}{M},1\right] \end{cases} \tag{16}$$

Thus, in the low r regime, each source in the cooperative network achieves the optimal $c(R,\underline{d})$ of an $M\times 1$ MIMO network given by (13), with dependence only on the distance of the M transmitting nodes to the destination. However, the range of r for which these optimal gains are achieved is dependent on the distance between the cooperating nodes with increasingly proximal cooperating nodes (larger Δ_{km}, and hence, $\kappa_m^{(\mathcal{C})}$) achieving correspondingly larger ranges. Finally, in the high r regime, $c_m(R,\underline{d})$ depends on all the relevant inter-node distances.

5 Illustration of Results

Consider an $M=2$ cooperative network with a collinear geometry as shown in Fig. 1. As with the MIMO case, the transmit node N_1 is fixed at the origin a unit distance from the destination node N_3. The cooperating node, denoted by N_2, is at a distance $d\in[0,1]$ from N_1. Unlike the 2×1 distributed MIMO network where both nodes cooperate fully, in the cooperative network employing the DDF strategy, node N_2 aids N_1 only after it has decoded the signal from N_1. As before, N_1 and N_2 transmit with the same average power such that their SNR at any receiver is ρ. We plot the outage probability curves for this network as a function of ρ for two choices of the path-loss exponent, $\alpha=2$ and $\alpha=4$ and a fixed rate $R=1$. For this fixed R, as ρ increases, the corresponding multiplexing gain r decreases approaching 0 in the limit.

In Fig. 3, subplot A, for $R=1$ and $\alpha=4$, we plot the outage probability curves as a function of the SNR ρ, one for each choice of the distance d between the two nodes. The curves plotted are obtained via Monte Carlo simulations. Observe the outage curves match those for the 2×1 distributed MIMO network in Fig. 2 for placement of N_2 at $-.25$, $.01$, $.25$ where N_2 is closer to N_1. However, contrary to the MIMO-like gains predicted in (16) for $r<.5$, the SNR gains for the chosen SNR range do not demonstrate a monotonic behavior with increasing d as in Fig. 2; instead they increase for $d\leq .5$ and then decrease. This is because, unlike the distributed MIMO network, in the cooperative network a fraction f of the total time or bandwidth resources is allocated at N_2 given as (see [5])

$$f = \min\left\{1, \frac{R}{\log(1+\rho\left|h_{12}\right|^2/\,d_{12}^{a})}\right\} = \min\left\{1, \frac{R}{\log(1+\rho^{1+\Delta_{12}-v_{12}})}\right\} \tag{17}$$

where v_{12} and Δ_{12} are the exponential orders of the channel gain $\left|h_{12}\right|^2$ and distance $d_{12}=d$, respectively, between N_1 and N_2. Thus, for a given realization h_{12}, N_2 receives signals from

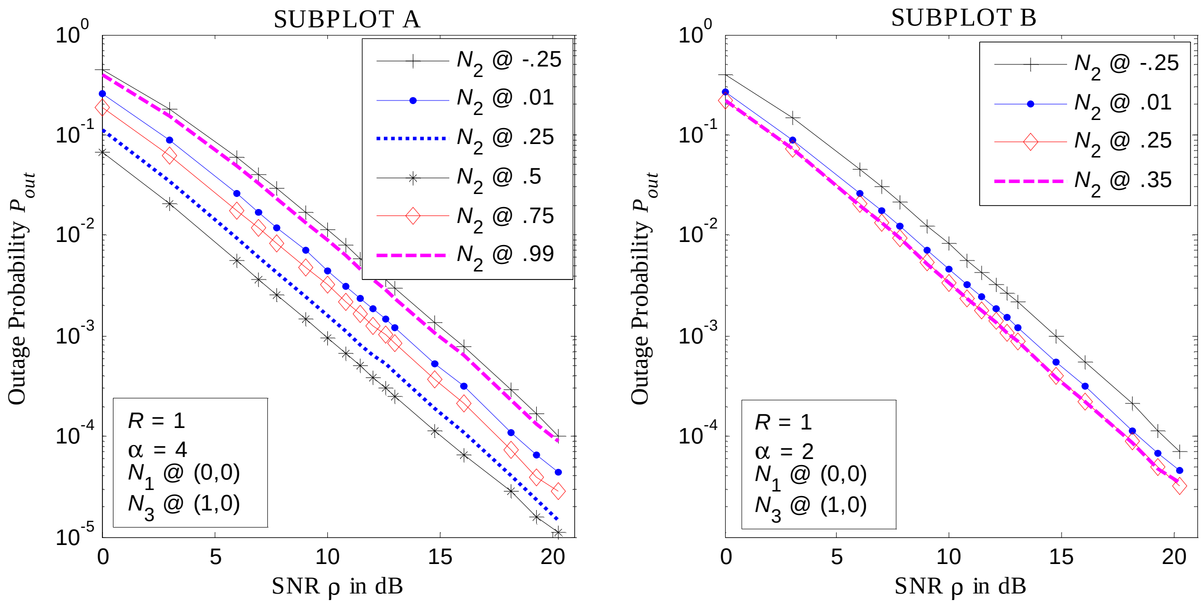

Figure 3: P_{out} for an $M = 2$ Cooperative Network for $(R = 1, \alpha = 4)$ and $(R = 1, \alpha = 2)$

N_1 over fl symbols until it successfully decodes the source message. An outage occurs when the transmit rate R is greater than the destination rate

$$R_d = f \log\left(1 + \frac{\rho\,|h_{13}|^2}{d_{13}^a}\right) + (1-f)\log\left(1 + \frac{\rho\,|h_{13}|^2}{d_{13}^a} + \frac{\rho\,|h_{23}|^2}{d_{23}^a}\right). \tag{18}$$

For a given ρ, the path-gains inclusive SNR at N_2, ρ/d_{12}^{α}, increases with decreasing d. This in turn results in f in (17) taking decreasing values on average. On the other hand, the second $\log(\cdot)$ term in R_d that results from cooperation, say R_c, increases with increasing d since $d_{23} = 1 - d$. The non-monotonic behavior of the outage probability curves in Fig. 3, subplot A, then reflects the combined effect of d on $(1-f)$ and R_c for $R = 1$. The corresponding outage curves for the same R and $\alpha = 2$ are plotted in subplot B. In addition to depending on the distance, we now observe that the path-gains inclusive SNR also depends on the path-loss exponent α. Since the path-gain inclusive SNR increases with α for $d \in [0, 1]$, we expect that the range of d for which the high SNR approximation holds for $\alpha = 2$ to be smaller. This is confimed in Fig. 3 where the MIMO-like behavior now reverses at $d = .25$.

From Figure 3, subplot A, we further conclude that for the relatively low SNR range considered, the outage probability and the SNR gains predicted in (16) hold only for $d < .5$. It can be shown that the observed SNR gains differ from the predicted gains as d increases beyond $.35$. For a fixed R, as ρ increases, from (17), we expect that the mean value of F for any d will decrease. This in turn will increase the range of d for which the high SNR approximation applies. We demonstrate this in Fig. 4 where in subplot A we compare the probability distribution of the fraction F at $d = .25$ and $d = .75$ for $\rho = 20$ dB. The corresponding comparison for $\rho = 80$ dB is shown in subplot B. We observe here that for a given ρ, the mean and variance of F increases with increasing d. However, as ρ increases, the “difference” in the distribution of F for different d becomes negligible as shown in subplot B. Thus, at 80 dB, where the effect of F on (18) is negligible, the MIMO-like SNR gains predicted in (16) will be valid for both $d = .25$ and $d = .75$ unlike at 20 dB where it does not hold for $d = .75$.

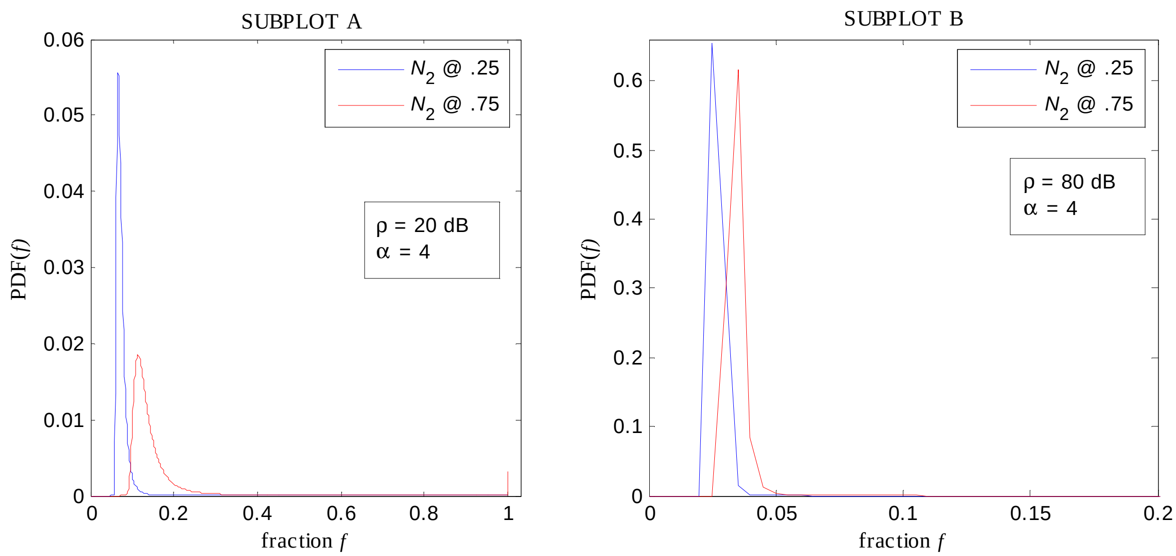

Figure 4: Probability Distribution Function of fraction f for different choices of ρ and d

The above examples suugests that the asymptotic geometry-inclusive error analysis is applicable when the SNR ρ is above a certain threshold $\mathsf{T}_{\mathsf{SNR}}(\underline{d}, R, \alpha)$ that is also a function of R, $\underline{d}$, and α. For the $M = 2$ cooperative network considered above, clearly $\mathsf{T}_{\mathsf{SNR}}(\underline{d}, R, \alpha)$ increases with increasing d for a fixed R and α. Further, the plots also indicate that to achieve optimal MIMO-like SNR gains it is desirable to choose the node closest to the destination as the cooperating node or relay, subject to $\rho \geq \mathsf{T}_{\mathsf{SNR}}(\underline{d}, R, \alpha)$. Thus, for the asymmetric cooperative network considered in Fig. 1 where N_2 is closer to N_3 than N_1, while both nodes achieve the maximum diversity gains of 2 via cooperation, N_1 also enjoys an SNR advantage relative to N_2. Similar comparisons can also be made for cooperative networks with $M > 2$. For each such network, the requirement of decoding at one or more nodes will determine an appropriate $\mathsf{T}_{\mathsf{SNR}}(\underline{d}, R, \alpha)$ beyond which the predicted SNR gains in (16) hold.

6 Concluding Remarks

We have presented an approach to evaluate the geometry-inclusive asymptotic outage probability for a variety of networks. For wireless networks where node cooperation yields large diversity gains, and a corresponding increase in reliability, the analysis highlights the effect of exploiting network geometry to also achieve SNR gains. Such SNR based comparisons might also help choose between network architectures such as cooperative networks or relay-based hierarchical networks [7]. Finally, the analysis can also be applied to other strategies such as amplify-and-forward.

References

[1] E. Telatar, "Capacity of multi-antenna Gaussian channels," *Europ. Trans. Telecommunications*, vol. 10, pp. 585–595, Nov. 1999.

[2] G. J. Foschini and M. J. Gans, “On limits of wireless communications in a fading environment when using multiple antennas,” *Wireless Personal Comunications: Kluwer Academic*, vol. 6, no. 3, pp. 311–355, Mar. 1998.

[3] A. Sendonaris, E. Erkip, and B. Aazhang, “User cooperation diversity - part I: System description,” *IEEE Trans. Commun.*, vol. 51, no. 11, pp. 1927–1938, Nov. 2003.

[4] J. N. Laneman, D. N. C. Tse, and G. Wornell, “Cooperative diversity in wireless networks: efficient protocols and outage behavior,” *IEEE Trans. Inform. Theory*, vol. 50, no. 12, pp. 3062–3080, Dec. 2004.

[5] K. Azarian, H. El Gamal, and P. Schniter, “On the achievable diversity-multiplexing tradeoff in half-duplex cooperative channels,” July 2004, preprint.

[6] L. Zheng and D. N. C. Tse, “Diversity and multiplexing: A fundamental tradeoff in multiple-antenna channels,” *IEEE Trans. Inform. Theory*, vol. 49, no. 5, pp. 1073–1096, May 2003.

[7] L. Sankaranarayanan, G. Kramer, and N. B. Mandayam, “Cooperation vs. hierarchy: An information-theoretic comparison,” in *Int. Symp. Inf. Theory*, Adelaide, Australia, Sept. 2005.

[8] J. N. Laneman, “Network coding gain of cooperative diversity,” in *Proc. IEEE Military Comm. Conf. (MILCOM)*, Monterey, CA, Nov 2004.

[9] T. H. Cormen, C. E. Leiserson, and R. L. Rivest, *Introduction to Algorithms*. Cambridge, MA: The MIT Press, 1990.

[10] A. Host-Madsen, “On the capacity of wireless relaying,” in *IEEE Vehicular Tech. Conf.*, Vancouver, CA, Sept. 2002.

[11] G. Kramer, “Models and theory for relay channels with receive constraints,” in *42nd Annual Allerton Conf. on Commun., Control, and Computing*, Monticello, IL, Sept. 2004.